ARTICLE OPEN

Check for updates

Gottesman-Kitaev-Preskill qubit synthesizer for propagating light

Kan Takase[1,2]✉, Kosuke Fukui[1], Akito Kawasaki[1], Warit Asavanant[1,2], Mamoru Endo[1,2], Jun-ichi Yoshikawa[2], Peter van Loock[3] and Akira Furusawa[1,2]✉

Practical quantum computing requires robust encoding of logical qubits in physical systems to protect fragile quantum information. Currently, the lack of scalability limits the logical encoding in most physical systems, and thus the high scalability of propagating light can be a game changer. However, propagating light also has difficulty in logical encoding due to weak nonlinearity. Here, we propose a synthesizer that encodes Gottesman-Kitaev-Preskill (GKP) qubits in propagating light by exploiting the nonlinearity of photon detectors. This synthesizer is based on an approach what we call Gaussian breeding, leading to the following four advantages: (i) systematic and rigorous synthesis of arbitrary GKP qubits, (ii) use of minimal resources, (iii) high fidelity and high success probability, and (iv) robustness against loss. There has been no protocol that incorporates all these advantages, and thus the proposed synthesizer excels in both performance and feasibility. By employing our method, one can generate GKP qubits using a few to several squeezed light sources, beam splitters and photon detectors.

npj Quantum Information (2023)9:98 ; https://doi.org/10.1038/s41534-023-00772-y

INTRODUCTION

Quantum computers are expected to outperform classical computers in certain tasks. For quantum computers to become a technology that changes our lives, it is necessary to protect fragile quantum information and ensure the reliability of computation. The basic idea for this is to encode quantum information redundantly as a logical qubit in a high-dimensional Hilbert space[1,2]. However, encoding of logical qubits is typically challenging for any physical system, for different reasons. For example, scalability is a critical issue in stationary two-level systems, because each logical qubit should be encoded in a quantum many-body system. A logical qubit with high redundancy is encoded in 10^3 to 10^4 physical qubits, and millions or more physical qubits are required to perform practical tasks[3]. Spatial parallelization and control of such a large number of physical qubits are far beyond the current techniques that deal with tens to hundreds of physical qubits[4,5].

For avoiding the problem of scalability, encoding a qubit in an oscillator is a promising approach. Each logical qubit can be encoded in just one oscillator thanks to its infinite-dimensional Hilbert space. Thus, we can realize robust encoding by concatenating a reasonable number of qubits in oscillators. A prime example is the Gottesman-Kitaev-Preskill (GKP) qubit[6]. The GKP qubit is a powerful logical qubit, due to its intrinsic robustness, living in a quantum error correction code space. Ideally, the GKP qubit is a superposition of equally-spaced position eigenstates, but is usually approximated as a superposition of squeezed coherent states, as shown in Fig. 1a. Given data qubits and ancillary magic states, which is GKP qubits with a special superposition coefficient, fault-tolerant and universal quantum computing is possible using only linear operations on position and momentum, which are called Gaussian operations[6–10].

Quantum computation using GKP qubits can be defined in any type of quantum harmonic oscillator, but the challenges for its realization vary greatly depending on the physical system. Although it is relatively easy to generate GKP qubits in nonlinear systems such as trapped ions[11] and superconducting circuits[12], interacting the generated qubits for quantum computing is difficult. The reason is that the qubits are localized apart as matter or standing waves, so they are difficult to have any interactions. In addition, the cost of Gaussian operations necessary for the logical operation on GKP qubits is high due to intrinsic nonlinearity of the system. In contrast, in propagating light, GKP qubits are difficult to generate but easy to use. A scalable platform that can input multiple GKP qubits and perform arbitrary Gaussian operations has already been demonstrated[13–16]. Therefore, generation of GKP qubits in propagating light is one of the most desired breakthroughs for realizing practical quantum computers.

The obstacles preventing the generation of GKP qubits is the lack or weakness of natural nonlinearity of propagating light. Although it is known that matter-light[11,12] or light-light[6] nonlinear interactions enable logical encoding, they are challenging to realize in propagating light. A promising approach to circumvent this is to leverage the nonlinearity of photon detectors, which has been widely used experimentally[17–20]. How to exploit the nonlinearity of the photon detectors for the logical encoding, however, is a highly nontrivial questions and have been a topic of current researches. One approach is a cat breeding protocol[21,22] that utilizes interference of multiple Schrödinger cat states and homodyne measurements. In this protocol, it is necessary to prepare initial cat states with large amplitudes, as the intervals between the superimposed squeezed coherent states decrease with each breeding steps. Generating such cat states requires the detection of a large number of photons, easily exceeding hundreds in total. Additionally, this protocol only allows for the generation of specific codewords of the GKP qubits. Another approach to generate GKP qubits based on Gaussian Boson sampling has also been recently investigated[23–26] as it is expected

[1]Department of Applied Physics, School of Engineering, The University of Tokyo, 7-3-1 Hongo, Bunkyo-ku, Tokyo 113-8656, Japan. [2]Optical Quantum Computing Research Team, RIKEN Center for Quantum Computing, 2-1 Hirosawa, Wako, Saitama 351-0198, Japan. [3]Institute of Physics, Johannes-Gutenberg University of Mainz, 7 Staudingerweg, 55128 Mainz, Germany. ✉email: takase@ap.t.u-tokyo.ac.jp; akiraf@ap.t.u-tokyo.ac.jp

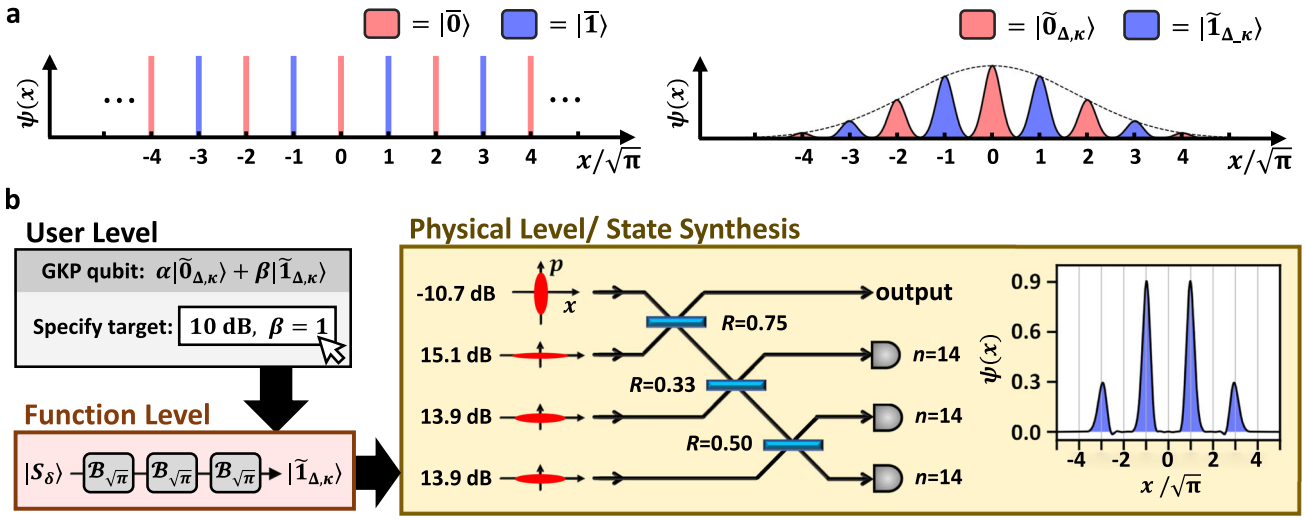

Fig. 1 Schematic of the GKP qubit synthesizer. a Wave functions of GKP qubits. Ideal codewords $|\bar{0}\rangle, |\bar{1}\rangle$ are a superposition of position eigenstates spaced by $2\sqrt{\pi}$. The approximated codewords $|\tilde{0}_{\Delta,\kappa}\rangle, |\tilde{1}_{\Delta,\kappa}\rangle$ are a superposition of squeezed states (variance $1/2\Delta^2$) with a Gaussian envelope (variance $\kappa^2/2$). **b** A synthesis example. As a user sets a target, the generation procedure is decided by combining basic functional blocks. Then, an actual circuit that can generate the target is derived. This protocol can synthesize arbitrary GKP qubits systematically.

to be more advantageous than the cat breeding protocols in terms of resource requirements. The experimental requirements are expected to be minimal as the sytem consists only of experimentally accessible elements, single-mode squeezed states and beam splitters, in addition to the photon detectors. A downfall of this approach is that parameters of the Gaussian Boson sampling system for the GKP qubit generations must be determined numerically. This problem, however, is complex enough to exhibit quantum supremacy[19,20], making it unrealistic to find parameters in the general case. Even if we restrict the target state to the standard Pauli codewords, only solutions have been found that either give limited error correction capability or have a very low generation rate.

Here, we propose a GKP qubit synthesizer that can generate an arbitrary superposition state of GKP qubits with high fidelity and high generation rate. Figure 1b is an operating image. When a user specifies a GKP qubit with arbitrary superposition coefficients, the synthesis procedure is given as a combination of abstract functional blocks. Then, by converting each functional block into a physical circuit and simplifying the whole circuit, the actual synthesis system having Gaussian Boson sampling configuration will be specified. These procedures are so easy that an actual experimental setup like Fig. 1b can be readily derived even by calculations by hand. Our formulation allows to incorporate the benefits of two distinct state-generation methods while circumventing their drawbacks: it is systematic and comprehensible like the cat-state breeding protocol and resource saving like the Gaussian Boson sampling as a state synthesizer. For this reason, we can refer to our protocol as Gaussian breeding. Note that Gaussian breeding can be achieved with fewer resources than Gaussian Boson sampling. For example, only three beam splitters are used in 1b, whereas six beam splitters are used in a Gaussian Boson Sampling of the same size. In addition, Gaussian breeding exhibits robustness against photon losses in that state deterioration due to photon loss does not accumulate so much even if the system scale becomes large. These features show that our GKP synthesizer based on Gaussian breeding is highly feasible and a practical breakthrough in the development of optical quantum computers.

RESULTS

Basic functional blocks of GKP qubit synthesis

The first step in GKP qubit synthesis is to build a diagram like Fig. 2a using functional blocks. Since the GKP qubit has a characteristic periodical wavefunction, it is not difficult to clarify the synthesis procedure by combining functional blocks that have specific effects on the wavefunction. For example, if the codewords of qubits are the target, the desired state can be synthesized by "bifurcating" one Gaussian wavefunction iteratively, as shown in Fig. 2b. We leave the physical realization of the basic functions like bifurcation to the next section, and in this section we discuss how to synthesize the GKP qubits at the functional block level.

First, we show the definition of the GKP qubit. In the following, we suppose that the position and momentum operators satisfy a commutation relation $[\hat{x}, \hat{p}] = \mathrm{i}$. For simplicity, normalization is omitted in the notation of quantum states below. We denote a squeezed vacuum state by $|S_\Delta\rangle = \hat{S}(\Delta)|0\rangle = \mathrm{e}^{\frac{\mathrm{i}\ln\Delta}{2}(\hat{x}\hat{p}+\hat{p}\hat{x})}|0\rangle$, where the squeezing operator gives $\hat{S}^\dagger(\Delta)\hat{x}\hat{S}(\Delta) = \Delta\cdot\hat{x}$ and $|0\rangle$ is the single-mode vacuum state. The physical codewords of GKP qubits $|\tilde{k}_{\Delta,\kappa}\rangle$ $(k = 0, 1)$ are

$$|\tilde{k}_{\Delta,\kappa}\rangle = \left[\sum_{s=-\infty}^{\infty} \mathrm{e}^{-\frac{\kappa^2}{2}((2s+k)\sqrt{\pi})^2}\hat{D}\big((2s+k)\sqrt{\pi}\big)\right]|S_\Delta\rangle, \tag{1}$$

where $\hat{D}(d) = \mathrm{e}^{-\mathrm{i}d\hat{p}}$ $(d \in \mathbb{R})$ is a position shift operator. These codewords approach the ideal GKP codewords in the limit of $\Delta, \kappa \to 0$.

The functional blocks we need are *coherent bifurcation* and *damping*. Coherent bifurcation $\mathcal{B}_w[\cdot]$ $(w \in \mathbb{R})$ generates a superposition of displaced squeezed vacuum states. This operator satisfies

$$\mathcal{B}_w\big[\hat{D}(d)|S_\Delta\rangle\big] = \big[\hat{D}(d-w) + \hat{D}(d+w)\big]|S_\Delta\rangle, \tag{2}$$

$$\mathcal{B}_w[a|\psi\rangle + b|\phi\rangle] = a\mathcal{B}_w[|\psi\rangle] + b\mathcal{B}_w[|\phi\rangle]. \tag{3}$$

We denote an N-times iteration of coherent bifurcation as $\mathcal{B}_w^{(N)}$,

$$\mathcal{B}_w^{(N)}[|\psi\rangle] = \mathcal{B}_w\Big[\mathcal{B}_w^{(N-1)}[|\psi\rangle]\Big],\ \mathcal{B}_w^{(0)}[|\psi\rangle] = |\psi\rangle. \tag{4}$$

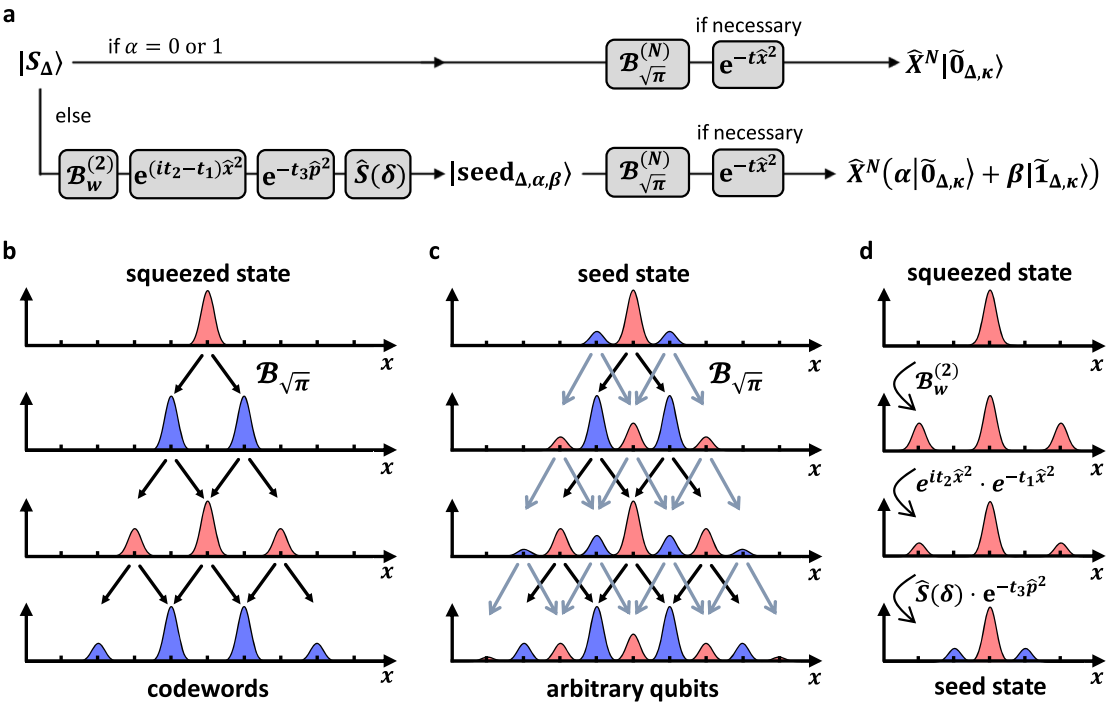

Fig. 2 Functional block diagram. a The diagram for the synthesis of arbitrary GKP qubits which consists of coherent bifurcation, damping, and Gaussian oeprations. **b** Changes in the wavefunction during the synthesis of codewords from a squeezed state. **c** Generation of arbitrary GKP qubits by using the seed state as an initial state. **d** Generation of a seed state from a squeezed state using coherent bifurcation, damping, and Gaussian operations. This diagram shows the case of $w = \sqrt{\pi}$.

A damping function is given by an operator $e^{-t\hat{x}^2}$ ($e^{-t\hat{p}^2}$), which decreases the energy of a quatum state by multiplying a Gaussian envelope e^{-tx^2} (e^{-tp^2}) to the wave function of x (p).

Let us consider synthesis of the codewords $|\tilde{0}_{\Delta,\kappa}\rangle, |\tilde{1}_{\Delta,\kappa}\rangle$. As shown in Fig. 2b and Methods, the GKP codewords can be obtained from a squeezed vacuum state via suitable N-times coherent bifurcation,

$$\mathcal{B}^{(N)}_{\sqrt{\pi}}[|S_\Delta\rangle] \approx \hat{X}^N \left|\tilde{0}_{\Delta,1/\sqrt{N\pi}}\right\rangle, \tag{5}$$

where $\hat{X}$ is a logical bit-flip operator. Note that the parity of iteration N decides the parity of the output, $|\tilde{0}_{\Delta,\kappa}\rangle$ or $|\tilde{1}_{\Delta,\kappa}\rangle$. If necessary, the value $\kappa = 1/\sqrt{N\pi}$ can be adjusted to a smaller value by applying a damping operation. Then, the functional diagram is given by Fig. 2a. More specifically, let us consider the case shown in Fig. 1b where a user wants to generate $|\tilde{1}_{\Delta,\kappa}\rangle$ with 10 dB squeezing. The initial state is a squeezed vacuum state around 10 dB, $|S_\delta\rangle$. The value of N should be odd, and adopted $N = 3$ as it is enough to approximates a 10 dB codeword. We can adjust the value $\kappa \approx 1/\sqrt{N\pi}$ by damping, but this is omitted here.

Coherent bifurcation and damping are also useful in synthesizing arbitrary GKP qubits. Arbitrary GKP qubits can be generated from a seed state defined by

$$|\mathrm{seed}_{\Delta,\alpha,\beta}\rangle = \alpha|S_\Delta\rangle + \frac{\beta}{2} \cdot \mathcal{B}_{\sqrt{\pi}}[|S_\Delta\rangle], \tag{6}$$

where $|\alpha|^2 + |\beta|^2 = 1$. By applying an appropriate $\mathcal{B}^{(N)}_w$, now we get

$$\mathcal{B}^{(N)}_{\sqrt{\pi}}\left[|\mathrm{seed}_{\Delta,\alpha,\beta}\rangle\right] \approx \hat{X}^N \left[\alpha \left|\tilde{0}_{\Delta,\sqrt{N\pi}}\right\rangle + \beta \left|\tilde{1}_{\Delta,\sqrt{N\pi}}\right\rangle\right], \tag{7}$$

as shown in Fig. 2c and Methods. Figure 2d shows a possible procedure of seed state generation with $|\alpha| \geq |\beta|$ using coherent bifurcation, damping, and a quadratic phase gate $e^{it\hat{x}^2}$,

$$|\mathrm{seed}_{\Delta,\alpha,\beta}\rangle \approx \hat{S}(\delta) \cdot e^{-t_3\hat{p}^2} \cdot e^{it_2\hat{x}^2} \cdot e^{-t_1\hat{x}^2} \cdot \mathcal{B}^{(2)}_w[|S_\Delta\rangle] \quad (w \geq \sqrt{\pi}/2), \tag{8}$$

with certain t_1, t_2, t_3 and δ given in Methods. The approximation gets better as w increases. Therefore, at the functional level, arbitrary GKP qubits can be synthesized according to the procedure shown in Fig. 2a.

Derivation of physical circuits

Here, we introduce how the abstract diagram of Fig. 2a translates to a physical circuit of propagating light. In systems other than optical traveling waves, bifurcation operations can be realized by nonlinear interactions between oscillators and two-level systems. Codewords of GKP qubits have been generated in trapped ions[11] and superconducting circuits[12] by using this type of interaction. Since such nonlinear operations are not viable option in propagating light, we propose a completely different methodology using the nonlinearity of photon number measurements. Derivation of the physical circuit is performed in the following two steps. First, we clarify how to implement coherent bifurcation and damping only using squeezed vacuum states, Gaussian operations, and photon number measurements. Next, a circuit combining these functional blocks is readily transformed to a highly feasible circuit that consists of squeezed vacuum states, beam splitters, and photon number measurements as shown in Fig. 1b.

In order to understand how to realize coherent bifurcation, we decompose Eq. (2) into two equations,

$$\mathcal{B}_w[|S_\Delta\rangle] = \left[\hat{D}(-w) + \hat{D}(w)\right]|S_\Delta\rangle, \tag{9}$$

$$\mathcal{B}_w\left[\hat{D}(d)|S_\Delta\rangle\right] = \hat{D}(d)\mathcal{B}_w[|S_\Delta\rangle]. \tag{10}$$

Equation (9) is realized by a generalized photon subtraction[27], a method for creating Schrödinger cat states. Figure 3a shows the setup, where two squeezed vacuum states $|S_{\Delta_1}\rangle_1$ and $|S_{\Delta_2}\rangle_2$ interact by a beam splitter interaction $\hat{B}$ with transmittance $T = 1 - R$ followed by the detection of n photons. Any n is useful, but below we assume n is even. This process $\mathcal{G}_w$ well

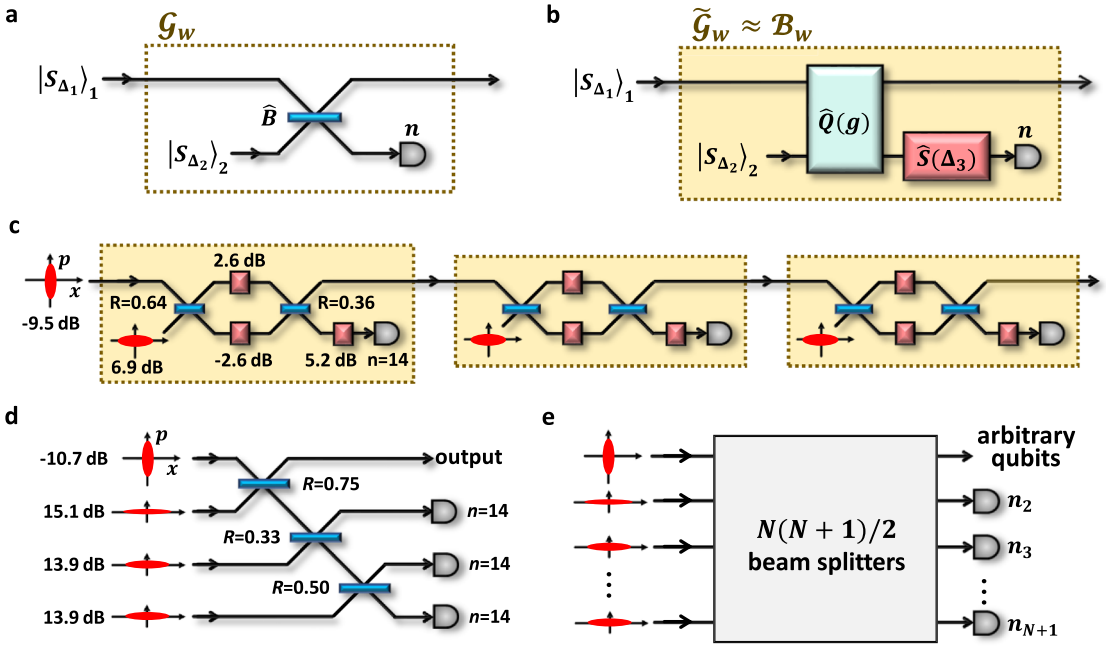

Fig. 3 Physical circuits of basic functions and the whole setup. a A setup of the generalized photon subtraction. Squeezed Schrödinger cat states are generated from squeezed states. **b** The setup of the iterable generalized photon subtraction using a quantum-non-demolition interaction. It implements the coherent bifurcation and the damping operation only with the help of a Gaussian ancillary state, Gaussian operations, and a photon number measurement. **c** A naive implementation of the synthesis of $|\tilde{1}_{\Delta,\kappa}\rangle$ with 10 dB squeezing by iterating three coherent bifurcation. We assume that the same parameters are used in all bifurcation processes. **d** An equivalent circuit of (**c**) derived from the Bloch-Messiah reduction. **e** General setup for arbitrary GKP qubit synthesis. When N detectors are used, it requires $N(N+1)/2$ beam splitters at most.

approximates Eq. (9),

$$\mathcal{G}_w[|S_\Delta\rangle] \approx \left[\hat{D}(-w)+\hat{D}(w)\right]|S_\Delta\rangle,\ w=\sqrt{2n}\Delta, \tag{11}$$

when $n \geq 2$, $T\Delta_1^{-2}+R\Delta_2^{-2}=1$ and $\Delta_2^{-2}=1/(1+\Delta_1^{-2})$ (see Methods). Compared to conventional photon subtraction[28], the generalized photon subtraction can achieve a larger w for the same n with a much higher success probability, which indicates that the nonlinearity of the photon detector is efficiently exploited. Unfortunately, though, $\mathcal{G}_w$ does not in general implement $\mathcal{B}_w$, because the non-commutativity $\left[\hat{D}_1(d),\hat{B}\right]\neq 0$ leads to

$$\mathcal{G}_w\left[\hat{D}(d)|S_\Delta\rangle\right] \neq \hat{D}(d)\mathcal{G}_w[|S_\Delta\rangle], \tag{12}$$

which contradicts Eq. (10). We can avoid this problem by using a different interaction. We propose the iterable generalized photon subtraction $\tilde{\mathcal{G}}_w$ in Fig. 3b, where the beam splitter is replaced by a quantum-non-demolition (QND) interaction $\hat{Q}(g)=e^{ig\hat{p}_1\hat{x}_2}$ and $\hat{S}_2(\Delta_3)$. The QND interaction is a fundamental entangling gate and is commonly utilized for QND measurements of position and momentum. Since $\left[\hat{S}_2(\Delta_3)\hat{Q}(g),\hat{D}_1(d)\right]=0$, now we do get

$$\tilde{\mathcal{G}}_w\left[\hat{D}(d)|S_\Delta\rangle\right] = \hat{D}(d)\tilde{\mathcal{G}}_w[|S_\Delta\rangle], \tag{13}$$

as required according to Eq. (10). The operation $\tilde{\mathcal{G}}_w$ equivalently approximates Eq. (9) as $\mathcal{G}_w$ when $n \geq 2$, $\left(\Delta_2^{-2}+g^2\Delta_1^{-2}\right)\Delta_3^{-2}=1$ and $\Delta_1^2 \ll 1 \ll \Delta_2^2$ (see Methods). In the following, we put $c=\left(\Delta_2^{-2}+g^2\Delta_1^{-2}\right)\Delta_3^{-2}$. This process also obeys the linearity as shown in Eq. (3). As a result, $\tilde{\mathcal{G}}_w$ is an implementation of coherent bifurcation $\mathcal{B}_w$. This operation inherits the advantages of the generalized photon subtraction, such as large w, a high success probability, and a high fidelity. The theory of coherent bifurcation can be clearly described when $c=1$, but in practice the case $c\neq 1$ is also useful. According to generalized photon subtraction, the width of the bifurcation w increases at the expense of the fidelity of the output state when $c>1$, and vice versa when $c<1$. The parameter c will be an important degree of freedom in actual GKP state generation. Interestingly, this setup also realizes the damping operation $e^{-t\hat{p}^2}$ when $n=0$. We can further realize a damping about x by applying a $\pi/2$ phase rotation of the input and output states. Therefore, we are able to generate arbitrary GKP qubits by cascading the optical circuit in Fig. 3b.

Cascading the circuit in Fig. 3b, however, seems to pose an experimental challenge[29,30]. Let us consider again the example of Fig. 1b. A naive implementation of three coherent bifurcations is shown in Fig. 3c. A QND interaction is realized with two beam splitters and two online squeezers, so the whole circuit requires four squeezed vacuum states, six beam splitters, nine online squeezers, and three photon detectors. The parameters in Fig. 3c are set to satisfy $w=\sqrt{\pi}, c=1$ and $\Delta_1^2 \ll 1 \ll \Delta_2^2$. Implementation of such a complex circuit is difficult, where online squeezers are especially costful. Here, simplifying the circuit by Bloch-Messiah reduction[31] is useful. Bloch-Messiah reduction transforms a system of Gaussian states followed by Gaussian operations into single-mode squeezed states followed by beamsplitters. In the case of Fig. 3c, an equivalent circuit consists of four squeezed vacuum states, three beamsplitters, and three photon detectors as shown in Fig. 3d. This decomposition clearly increases the feasibility. So far we have considered a basic example, but the same methodology can be used to synthesize arbitrary GKP qubits. When N photon detectors are used, the diagram of Fig. 2a can be realized by at most $N(N+1)/2$ beam splitters[32], as shown in Fig. 3e. Note that while the setup in Fig. 3d, e has the same configuration as state generation using Gaussian Boson sampling, it is challenging to derive such a specific setup through numerical analysis as conventionally done. In our approach, we can efficiently reveal the desired setup by considering generation of superposition through generalized photon subtraction and the commutativity of the QND interaction and displacement operations. Additionally, in simple cases like generating standard Pauli

Table 1. Condition and results of the simulation.

Target state $\|target\rangle$	n	N	Success Probability	Squeezing $10\log_{10}\Delta^{-2}$ (dB)	Fidelity to $\hat{X}^N\|target\rangle$
$\|\tilde{0}_{\Delta,\Delta}\rangle$	6	2	1.06×10^{-3}	6.4	0.999
	6	3	5.75×10^{-5}	6.9	0.996
	10	3	1.65×10^{-5}	8.6	0.998
	10	4	6.12×10^{-7}	8.8	0.998
	16	3	5.05×10^{-6}	10.3	0.998
	16	4	1.18×10^{-7}	10.4	0.998
$\cos\frac{\pi}{8}\|\tilde{0}_{\Delta,\Delta}\rangle+\sin\frac{\pi}{8}\|\tilde{1}_{\Delta,\Delta}\rangle$	16	3	2.22×10^{-10}	10.2	0.997
	16	4	4.97×10^{-12}	10.6	0.998
$\frac{1}{\sqrt{2}}\|\tilde{0}_{\Delta,\Delta}\rangle+\frac{e^{-i\frac{\pi}{4}}}{\sqrt{2}}\|\tilde{1}_{\Delta,\Delta}\rangle$	16	3	3.53×10^{-10}	10.3	0.995
	16	4	8.06×10^{-12}	10.5	0.997
$\cos\theta\|\tilde{0}_{\Delta,\Delta}\rangle+e^{-i\frac{\pi}{4}}\sin\theta\|\tilde{1}_{\Delta,\Delta}\rangle*$	16	3	2.37×10^{-10}	10.3	0.996
	16	4	5.32×10^{-12}	10.4	0.997

$* \cos 2\theta = 1/\sqrt{3}$.
We simulate the generation of the codewords and three kinds of magic states. We numerically perform the coherent bifurcation on squeezed states or seed states N times. In each coherent bifurcation, n photons are detected and we assume $\sqrt{2n}\Delta_1 = \sqrt{\pi}$, $\Delta_2 = e, g = 1$, and $c = 1$. The value of Δ_2 is e in the case of codewords and $e^{1.16}$ in the case of magic states. Seed-state generation is simulated according to Eq. (8) with $w = \sqrt{\pi}$. The probability shows the total success probability including the generation of seed states.

codewords, we can generate GKP qubits using only a minimal number of beam splitters, specifically N beam splitters, instead of the $N(N+1)/2$ beam splitters typically assumed in Gaussian Boson sampling. This is a clear advantage that was not anticipated before.

Performance

We conduct numerical simulations of GKP-qubit generation in a Fock space up to 55 photons by using Strawberry Fields[33]. First, we simulate generation of the codewords $|\tilde{0}_{\Delta,\Delta}\rangle, |\tilde{1}_{\Delta,\Delta}\rangle$. We consider three cases where coherent bifurcation with $n = 6, 10, 16$ is iteratively employed. We perform a damping operation after iterating the bifurcation N times to increase the fidelity to the target states. Table 1 shows the results of the simulation. We can see that a smaller Δ is achieved by increasing the value of n. When $n = 16$, Δ is below $\sqrt{10}$ (10 dB squeezing), which is usually assumed as the fault-tolerant threshold[34]. All the simulated states have a high fidelity $F > 0.99$. The cat breeding protocol[21,22] can generate similar states by using different iterative oeprations, but each step reduces the interval between squeezed states by $1/\sqrt{2}$. As a result, the number of detected photons increases exponentially in cat breeding with the number of iterations, whereas it increases only linearly in our protocol. Let's consider achieving $\Delta \le \sqrt{10}$ in cat breeding. If we prepare cat states using generalized photon subtraction, we would need four cat states generated with detection of 64 photons for each, requiring detection of 256 photons in total. Furthermore, the success probability of such events is at most 2.0×10^{-10}, and achieving this would require squeezed light with $r = 2.8$ (24 dB). In a numerical analysis of state synthesizers based on Gaussian Boson sampling, $\Delta \le \sqrt{10}$ and a high fidelity $F > 0.999$ are achieved, but the success probability is kept as low as 10^{-29}[26]. On the contrary, if we aim to increase the generation success rate to around 10^{-6}, we currently only know of state generation systems that yield states with fidelities below 0.99 and error correction capabilities significantly below the target[25]. These comparisons indicate the high efficiency of our protocol. Figure 4a show how the wavefunctions of x and Wigner functions change by iterating coherent bifurcation with $n = 16$. It can be seen from the wavefunction that the protocol shown in Fig. 2b works. The Wigner functions illustrate the characteristics of GKP qubits that are often referred to as grid states.

For evaluation of this method, we calculate the success rate of quantum error correction using the synthesized $|\tilde{0}_{\Delta,\Delta}\rangle$ in the situation presented by Glancy and Knill[35]. In Fig. 4b, the rates obtained by the simulation are shown in a scatter plot, and the rates for the ideal states are shown in dashed lines. For the theoretical lines, we assume in Eq. (1) to take the summation from $s = -m$ to m and calculate the rate for $m = 0, 1, \infty$. The theoretical lines show that the more squeezed states are superimposed, the better the rate, and it is clearer when the squeezing level is high. Round dots are the results with $(n,N) = (4, 2), (4, 4), (6, 2), (6, 4), (10, 2), (10, 4), (16, 2), (16, 4)$ under the condition of $c = 1$. The star-shaped points are the result of $c = 0.8, 0.9, 1.1$ and 1.2 when $(n, N) = (16, 4)$. The larger the value of c, the higher the squeezing level, which is natural from the principles of generalized photon subtraction. Note that the fidelity F usually deteriorates as c increases, but here $F > 0.994$ is satisfied even when $c = 1.2$. The simulation results are in good agreement with the theoretical line of $m = \infty$, indicating that the synthesized states are of a high quality not only in fidelity but also in error correction capability. In particular, the high rate around 10 dB is a significant result that could not be verified in a previous study[25].

Next, we simulate generation of arbitrary GKP qubits $\alpha|\tilde{0}_{\Delta,\Delta}\rangle + \beta|\tilde{1}_{\Delta,\Delta}\rangle$. We target the three magic states[6–8] with $(\alpha,\beta) = \left(\cos\frac{\pi}{8}, \sin\frac{\pi}{8}\right), \left(\frac{1}{\sqrt{2}}, \frac{e^{-i\frac{\pi}{4}}}{\sqrt{2}}\right)$, and $\left(\cos\theta, \sin\theta e^{-i\frac{\pi}{4}}\right)$ where $\cos 2\theta = 1/\sqrt{3}$. Table 1 shows the simulation results. Magic states exceeding the fault-tolerant threshold are generated with a high fidelity $F > 0.99$. The success probability is smaller than for the case of codeword generation, because now we have to include the probability of generating seed states, which is about 10^{-5}. Figure 4c presents the Wigner functions of the simulated magic states. We can see that more complicated grid structures compared to the standard codewords can be successfully synthesized. The significance of this is that, in particular, resources of GKP magic states can be exploited to do universal quantum computation[9,10] by means of non-Clifford gate teleportation.

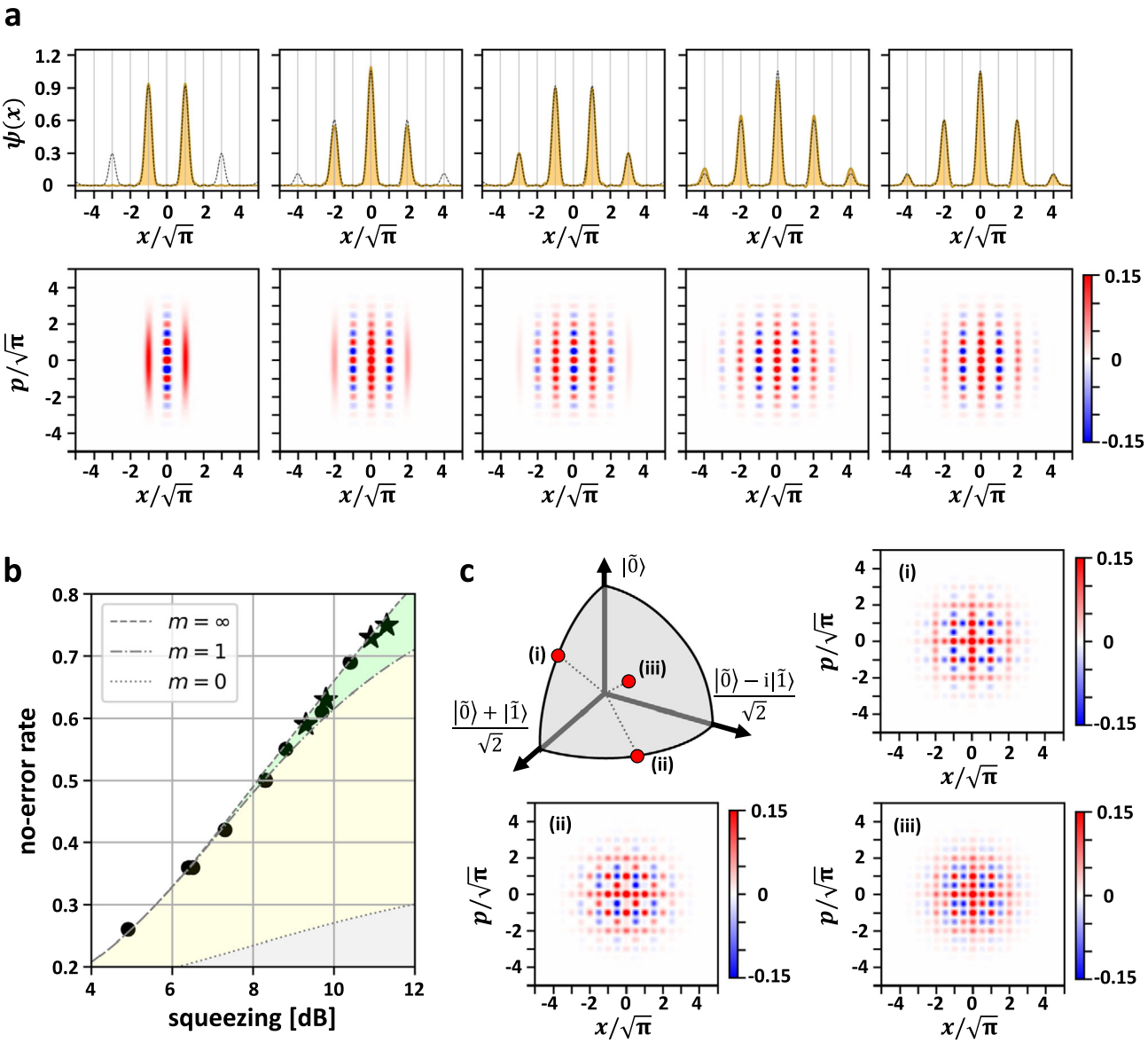

Fig. 4 Simulation of GKP qubit synthesis. a Wavefunctions and Wigner functions of the synthesized state with $n = 16$. From the left, $N = 1, 2, 3, 4$ and $N = 4$ followed by a damping operaiton. The broken lines are the wavefunctions of the target state. **b** No-error rate of theoretical and simulated $|\tilde{0}_{\Delta,\Delta}\rangle$ state. Round dots are the results with various (n, N) under $c = 1$. the star-shaped points are the result with $(n, N) = (16, 4)$ under $c \neq 1$. **c** Wigner functions of the synthesized magic states over 10 dB squeezing.

Robustness against loss

Here, we discuss the effect of photon loss, which is the most dominant experimental imperfection, and show the high feasibility of this protocol. In the simulation, we assume that the squeezers and the photon detectors have an efficiency η (loss $1-\eta$) in the beam splitter configuration of Fig. 3e. In general, photon loss degrades the generated state and reduces the success probability. Figure 5a, b show the evaluation of these effects for the cases of $n = 6$, 10, 16 and $N = 3$, 4. Figure 5a shows the deterioration of Wigner negativity due to photon loss. The volume of the negative part of a Wigner function is a standard indicator of quantum non-Gaussianity of a quantum state. The existence of non-zero Wigner logarithmic (log) negativity $W_{\log} = \log \int dxdp|W(x,p)|$ is necessary for universarity and quantum error correction of Gaussian errors[36,37]. It is difficult to discuss how much Wigner log negativity we need to demonstrate a GKP state generation, but here we assume that $W_{\log} > 0.2$ is the first experimental step to achieve. The reason is that when $W_{\log} > 0.2$ and $N = 3$, 4, more than 10% of the minimum value remains and we would be able to observe the negative area of the Wigner function. In that case, $\eta = 0.91$, 0.95, 0.97 or more are required for $n = 6$, 10, 16, respectively. The squeezer loss is less than 3% in the experiment that achieved the world record of −15 dB with optical parametric oscillator[38], and about 7% in the waveguide light source[39] compatible with photon number detectors. Photon detectors with less than 5% loss have also been reported[40,41]. For these reasons, the loss requirement for GKP qubit generation is within a realistic difficulty range. Figure 5b shows the success probability of state generation, showing that the success rate does not decrease so drastically. If the success probability is too low, state generation experiments become difficult. From the past state generation experiments[42,43], it is estimated that the experiment is possible even with the existing technology if the success rate is better than about 10^{-6}–10^{-4}. Therefore, in terms of success probability, experiments up to $N = 3$ and experiments

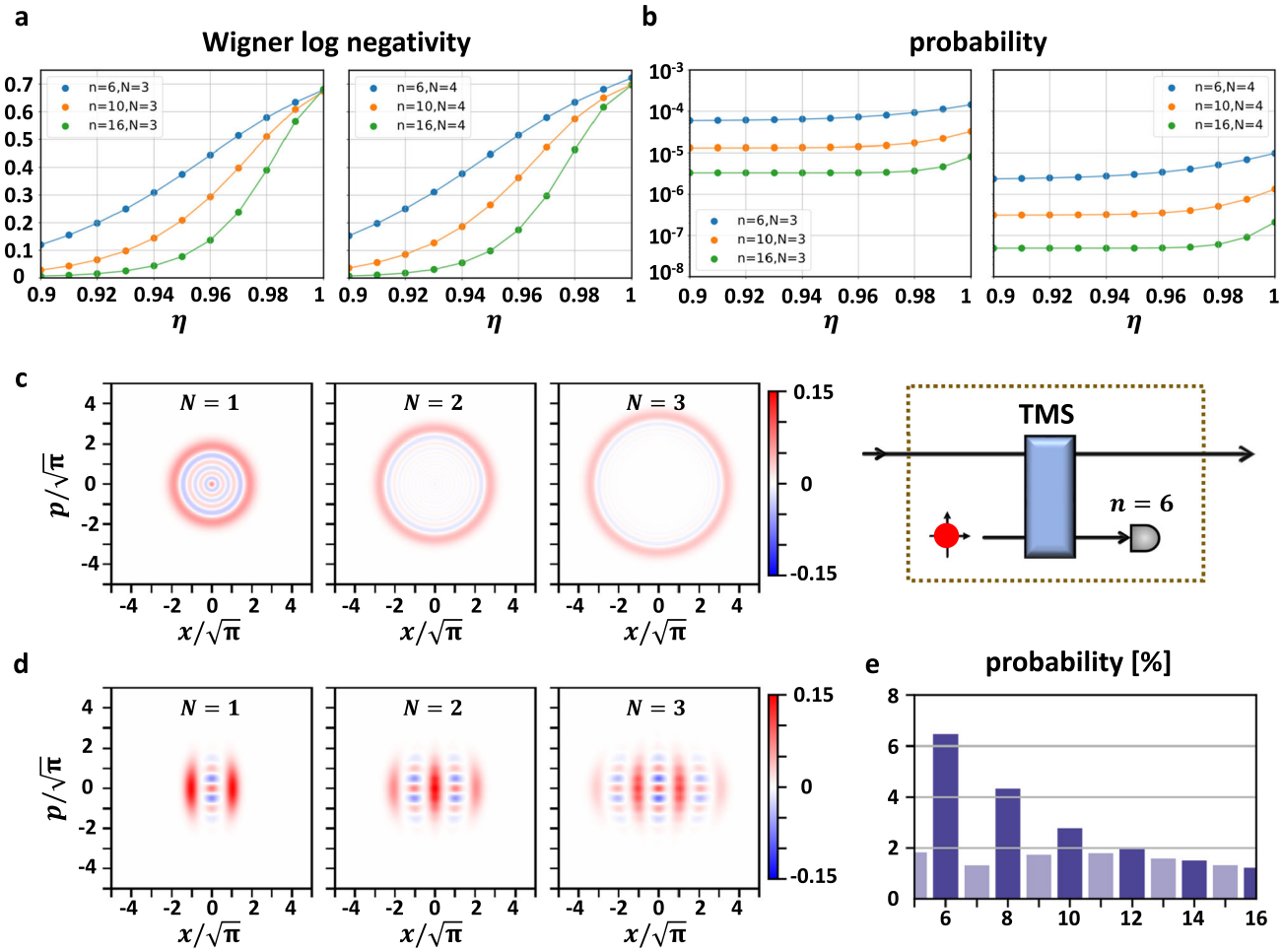

Fig. 5 Effect of photon loss. a Winger log negativity when the squeezers and the photon detectors have an efficienfy η. **b** Success probabilities under the same condition as (**a**). **c** Wigner functions obtained by iteration of photon addition with $\eta = 0.95$. The right side is the circuit of photon addition. The interaction strength was adjusted so that bifurcation operations in (**d**) and photon additions have similar success probabilities. TMS; two-mode squeezing. **d** Wigner functions given by iteration of coherent bifurcation with $\eta = 0.95$. **e** Probability to detect n photons in the third photon detector in the iteration of coherent bifurcation with $\eta = 1$. We assume that six photons were detected in the first and the second photon detectors.

with $N = 4$ and small n are already feasible. From the above, the generation of 7 dB GKP qubits that requires $(n, N) = (6, 3), (6, 4)$ is within the scope of existing technology. Generation of GKP qubits over 10 dB, including magic states, would also be feasible by improving photon loss and the rate of state generation.

The fact that 7 dB GKP qubits can be generated with current technology is an encouraging result for the realization of an optical quantum computer. For $(n, N) = (6, 3)$, detection of 18 photons is required in total, but a large photon loss of 9% is allowed in the squeezer and photon detectors, respectively. This makes us confident that this synthesizer may be loss tolerant to a certain extent. In fact, it has a desirable property: the quality of the generated states in a lossy environment is dominated by n rather than $n \times N$. Figure 5c, d show the Wigner functions that result from N iterations of $n-$photon addition and coherent bifurcation with $n = 6$, respectively. We assume that in both cases the state generation is conducted in a beam splitter configuration like Fig. 3e and the squeezers and the photon detectors have an efficiency $\eta = 0.95$. In the case of photon addition, both the log negativity and minimum value deteriorate as $(W_{\log}, W_{\min}) = (0.54, -0.030)$, $(0.36, -0.014), (0.26, -0.009), (0.21, -0.007)$ with $N = 1, 2, 3, 4$. In coherent bifurcation, on the other hand, the log negativity increases as $(W_{\log}, W_{\min}) = (0.17, -0.066), (0.32, -0.060), (0.45, -0.084)$, $(0.56, -0.074)$. Such a desirable property can be explained as follows. When $N = 3$, the number of detected photons in three steps is $(n_1, n_2, n_3) = (6, 6, 6)$ in both Fig. 5c, d. This event includes various possibilities, such as $(n_1, n_2, n_3) = (6, 7, 8)$ measured as $(6, 6, 6)$ due to photon loss. In the case of Fig. 5c, a state orthogonal to the target is generated, except when it is truly $(n_1, n_2, n_3) = (6, 6, 6)$. Since the probability of such a true event occurring is proportional to $\eta^{n_1+n_2+n_3}$, the quality of states such as fidelity and log negativity deteriorates as the total number of detected photons increases. On the other hand, the contamination due to the unexpected events is suppressed in the iteration of bifurcation, because even such events generate states somewhat close to the target. When there is no loss, the fidelity of the resulting states between $(n_1, n_2, n_3) = (6, 6, 6)$ and $(n_1, n_2, n_3) = (8, 6, 6), (6, 8, 6), (6, 6, 8)$ is 0.95, $(n_1, n_2, n_3) = (8, 8, 6), (8, 6, 8), (6, 8, 8)$ is 0.88, $(n_1, n_2, n_3) = (8, 8, 8)$ is 0.76. As N increases, the number of photon detection patterns that give states close to the target also increases. Thus, the quality of the generated state is less affected by N. Detection of an odd number of photons like $(n_1, n_2, n_3) = (6, 6, 7)$ gives a state orthogonal to the target, because it flips the parity of photon number components. Interestingly, such events are suppressed when $N \geq 2$. Figure 5e is the probability of obtaining $n_3 = n$ when $N = 3$, $(n_1, n_2) = (6, 6)$. and $\eta = 1$ is assumed. It shows that we are more likely to detect an even number of photons than an odd number of photons. This is because even n_3 leads to a constructive interference of wavefunctions like in Fig. 2b,

but odd n_3 leads to a destructive interference. The probability is given by $\int dx|\Psi(x)|^2$, where $\Psi(x)$ is an unnormalized wavefunction of a generated state, and thus n_3 is more likely to be even. As above, the proposed protocol has a non-accumulative property of photon loss, in which the state does not degrade even if a lossy circuit is iterated. Such robustness against photon loss is an important factor in the generation of complex states like GKP qubits.

DISCUSSION

This work provided a theoretical framework for systematically generating arbitrary GKP qubits in propagating light. At present, there are two directions for a further theretical improvement of this protocol. The first is optimization of various parameters. For simplicity, most of the simulations in the present research iterate exactly the same bifurcation. Experimental feasibility may be improved by using different parameters in each step. For example, by removing the constraint of detecting the same number of photons at each step, it could be possible to obtain the desired state with a smaller number of detected photons and a higher probability. Another important aspect is to improve the generation success probability using displacement. In the proposed method, the probability $P(k)$ of detecting k photons satisfies $P(k) > P(k+1)$, so the probability of detecting around 10 photons is at most several percent. However, since the displacement operation can remove this constraint, the success probability may be drastically improved. In fact, it is known that a quantum state called a cubic phase state can be generated quasi-deterministically by applying a displacement operation before photon number measurement[6]. Incorporating the displacement operation into the proposed method may lead to quasi-deterministic generation of GKP qubits.

In experiment, increasing the trial rate of state generation, which enables verification of state generation with lower success probability, is a straightforward direction. In recent years, the emergence of single-mode waveguide squeezers has made it possible, in principle, to generate high-purity states at a trial rate of 10 THz[39]. Thus, a success probability of 10^{-10} is high enough for demonstrating state generation, and even quasi-deterministic generation is possible by using a quantum memory with a reasonable life time of 1 ms[44]. In practice, the dead time of photon detectors would limit the trial rate. A transition edge sensor enables photon number resolving detection over 20 photons[17,45], but the existing sensors are slow and the trial rate is limited to several MHz[43]. Developing faster transition edge sensors[46] or use of superconducting nano wires for photon number resolving measurement[47–49], which can operate at 100 MHz, could be a possible solution. Even with these sub-GHz electronics, wavelength-division-multiplexed state generation[50] could exploit the full bandwidth of the squeezed light. Although the original proposal utilizes on-line nonlinear elements for wavelength conversion, quantum teleportation across different wavelength bands would be another feasible option. Reducing photon loss is also an essential research direction. Achieving fault tolerance would require much lower loss than demonstrating state generation. It is not easy to estimate the acceptable loss for fault tolerance, but numerical simulations of quantum error correction is one of the most feasible, applicable methods.

As mentioned in the introduction, the advantage of propagating light is that once the GKP qubits are generated, quantum computing can be readily performed. Therefore, it is important not only to pursue the generation of high-quality states, but also to actually perform multimode operations on the generated GKP qubits, which is demanding in other physical systems. For example, injecting GKP qubits into quantum processors or using them for demonstration of quantum error correction and non-Clifford operations are a meaningful application. The proposed synthesizer will enable such fundamental research on fault-tolerant quantum computing and will be a powerful driving force for the development of practical optical quantum computers.

Table 2. Summary of important notations.

Notation	Detail
Δ, κ	Factor of squeezing and Gaussian envelope of the GKP qubits
$\lvert\tilde{0}_{\Delta,\kappa}\rangle$, $\lvert\tilde{1}_{\Delta,\kappa}\rangle$	Physical codewords of the GKP qubits
$\mathcal{B}_w$	Ideal coherent bifurcation with a displacement factor w
$\mathcal{B}_w^{(N)}$	N-time iteration of $\mathcal{B}_w$
$e^{-t\hat{x}^2}$, $e^{-t\hat{p}^2}$	Damping operators of x and p
$\mathcal{G}_w$	Generalized photon subtraction
$\tilde{\mathcal{G}}_w$	Iterable generalized photon subtraction
c	A dominant parameter of the quality of $\tilde{\mathcal{G}}_w$
n	Detected photon number in each $\tilde{\mathcal{G}}_w$

METHODS

Important notations

We summarize the notations that appear in the main text in Table 2.

Coherent bifurcation

Here, we derive Eqs. (5) and (7). From the properties of $\mathcal{B}_w^{(N)}$, we get

$$\mathcal{B}_w^{(N)}[|S_\Delta\rangle] = \left[\sum_{l=0}^{N} {}_NC_l \cdot \hat{D}((2l-N)w)\right]|S_\Delta\rangle. \tag{14}$$

When $N \gg 1$, the binomial coefficient ${}_NC_l$ is well approximated by a Gaussian function,

$${}_NC_l \approx \sqrt{\frac{2^{2N+1}}{N\pi}}\exp\left(-\frac{2(l-N/2)^2}{N}\right). \tag{15}$$

When each displaced squeezed state in Eq. (14) is enough separated, we have

$$\left|\mathcal{B}_w^{(N)}[|S_\Delta\rangle]\right|^2 = \sum_{l=0}^{N} ({}_NC_l)^2 = {}_{2N}C_N \approx \frac{2^{2N}}{\sqrt{\pi}}. \tag{16}$$

When $N \gg 1$ and $w = \sqrt{\pi}$, we get

$$\begin{aligned}\tfrac{\sqrt[4]{\pi}}{2^N}\mathcal{B}_{\sqrt{\pi}}^{(N)}[|S_\Delta\rangle] &\approx \sqrt{\tfrac{2}{N\sqrt{\pi}}}\left[\sum_{l=0}^{N}\exp\left(-\tfrac{\left((2l-N)\sqrt{\pi}\right)^2}{2N\pi}\right)\cdot\hat{D}((2l-N)\sqrt{\pi})\right]|S_\Delta\rangle \\ &\approx \left|\tilde{k}_{\Delta,1/\sqrt{N\pi}}\right\rangle,\ k \equiv N\,(\mathrm{mod}\,2).\end{aligned} \tag{17}$$

The generation of arbitrary GKP qubits is confirmed from Eq. (17),

$$\begin{aligned}\sqrt{\tfrac{\sqrt{\pi}}{2^{2N}}}\mathcal{B}_{\sqrt{\pi}}^{(N)}[|\mathrm{seed}\rangle] &= \alpha\sqrt{\tfrac{\sqrt{\pi}}{2^{2N}}}\mathcal{B}_{\sqrt{\pi}}^{(N)}[|S_\Delta\rangle] + \beta\sqrt{\tfrac{\sqrt{\pi}}{2^{2(N+1)}}}\mathcal{B}_{\sqrt{\pi}}^{(N+1)}[|S_\Delta\rangle] \\ &\approx \hat{X}^N\left[\alpha\left|\tilde{0}_{\Delta,1/\sqrt{N\pi}}\right\rangle + \beta\left|\tilde{1}_{\Delta,1/\sqrt{N\pi}}\right\rangle\right].\end{aligned} \tag{18}$$

Damping operation

The damping operation is realized by supposing $n = 0$ in Fig. 3b, where $\hat{Q}(g) = e^{ig\hat{p}_1\hat{x}_2}$. When the input state is $|\psi_{\mathrm{in}}\rangle$, the output state is

$$|\Psi_{\mathrm{out}}\rangle_1 = {}_2\langle 0|\hat{S}_2(\Delta_3)\hat{Q}(g)|\psi_{\mathrm{in}}\rangle_1|S_{\Delta_2}\rangle_2. \tag{19}$$

Note that $|\Psi_{\rm out}\rangle_1$ is not normalized. The wave function of this state is

$$\begin{aligned}\Psi_{\rm out}(p_1) &= \int dp_2\, \psi_{\rm in}(p_1) \mathrm{e}^{-\frac{\Delta_2^2\Delta_3^2}{2}(p_2-\Delta_3^{-1}gp_1)^2}\cdot e^{-\frac{1}{2}p_2^2} \\ &= \sqrt{\frac{2\Delta_2^2\Delta_3^2}{1+\Delta_2^2\Delta_3^2}\pi}\,\psi_{\rm in}(p_1)\cdot\exp\left[-\frac{1}{2}\cdot\frac{g^2\Delta_2^2}{1+\Delta_2^2\Delta_3^2}p_1^2\right].\end{aligned} \tag{20}$$

This process therefore implements a damping operation $\mathrm{e}^{-t\hat{p}^2}$ with $t=\frac{g^2\Delta_2^2}{2(1+\Delta_2^2\Delta_3^2)}$. We can also realize a damping about x by applying a $\pi/2$ phase rotation of the input and output states.

The parameters in Eq. (8) explicitly are

$$t_1=\frac{1}{4w^2}\ln\left|\frac{\alpha}{\beta}\right|,\ t_2=\frac{1}{4w^2}\arg\left(\frac{\beta}{\alpha}\right),\ t_3=\frac{\Delta^2}{2}\left(\frac{4w^2}{\pi}-1\right),\ \delta=\frac{\sqrt{\pi}}{2w}. \tag{21}$$

In Eq. (8), we can omit the term $\hat{S}(\delta)\cdot\mathrm{e}^{-t_3\hat{p}^2}$ when $w=\sqrt{\pi}/2$, but more accurate seed states are obtained as w becomes larger than $\sqrt{\pi}/2$. This is because the term $\mathrm{e}^{it_2\hat{x}^2}\cdot\mathrm{e}^{-t_1\hat{x}^2}$, which is intended to multiply β/α to the displaced terms of $\mathcal{B}_w^{(2)}[|S_\Delta\rangle]=\left[\hat{D}(-2w)+2+\hat{D}(2w)\right]|S_\Delta\rangle$, works more accurately. Instead, we have to adjust the variance and displacement of the squeezed states when $w>\sqrt{\pi}/2$. The damping $\mathrm{e}^{-t_3\hat{p}^2}$ increases the variance of the squeezed states by convolving a Gaussian $\mathrm{e}^{-\frac{1}{4c}x^2}$ to the wave function about x. Finally, we get the desired state by applying $\hat{S}(\delta)$. Besides the generation of seed states, the damping operation also can be used to adjust the envelope of the GKP qubits. When $\Delta>1/\sqrt{N\pi}$, we can get square-lattice GKP qubits, $\mathrm{e}^{-t\hat{x}^2}[\alpha|\tilde{0}_{\Delta,\sqrt{N}w}\rangle+\beta|\tilde{1}_{\Delta,\sqrt{N}w}\rangle]\approx\alpha|\tilde{0}_{\Delta,\Delta}\rangle+\beta|\tilde{1}_{\Delta,\Delta}\rangle$, up to normalization by choosing a proper t.

Iterable generalized photon subtraction

The generalized photon subtraction[27] is a protocol to generate Schrödinger cat states. Figure 3a is the original setup defining the single-mode operation $\mathcal{G}_w$. We propose a setup in Fig. 3b as a different implementation defining the modified, adapted single-mode operation $\tilde{\mathcal{G}}_w$, which can be used for the Gaussian breeding. As the basic properties common to the both cases, the output state is given by

$$|\Psi_n\rangle_1={}_2\langle n|G\rangle_{1,2}, \tag{22}$$

where $|G\rangle_{1,2}$ is a two-mode Gaussian state. Note that $|\Psi_n\rangle_1$ is not normalized. The wave function $G(x_1,x_2)={}_2\langle x_2|_1\langle x_1|G\rangle_{1,2}$ can be an arbitrary Gaussian function but it is enough to assume the following form,

$$G(x_1,x_2)=\frac{|\sigma|^{\frac{1}{4}}}{\sqrt{\pi}}\exp\left[-\frac{1}{2}\boldsymbol{x}^T\sigma\boldsymbol{x}\right],\ \boldsymbol{x}=\begin{pmatrix}x_1\\x_2\end{pmatrix}, \tag{23}$$

where σ is a 2×2 real symmetric matrix. Assuming $\sigma_{22}=1$ makes it easier to handle this protocol analytically. First, we get

$$\Psi_n(x_1)=\left(\frac{|\sigma|}{\pi}\right)^{\frac{1}{4}}\frac{(-\sigma_{12})^n}{\sqrt{2^n n!}}x_1^n\exp\left(-\frac{1}{4\Delta_c^2}x_1^2\right), \tag{24}$$

$$\Delta_c^2=\frac{1}{|\sigma|+\sigma_{11}}. \tag{25}$$

The function in Eq. (24) is well approximated by superimposed Gaussian functions,

$$\mathcal{N}[\Psi_n(x_1)]\approx\mathcal{N}\left[\exp\left(-\frac{1}{2\Delta_c^2}\left(x_1-\sqrt{2n}\Delta_c\right)^2\right)+(-1)^n\exp\left(-\frac{1}{2\Delta_c^2}\left(x_1+\sqrt{2n}\Delta_c\right)^2\right)\right], \tag{26}$$

where $\mathcal{N}[\cdot]$ represents normalization. The fidelity of this approximation is

$$F_n=\frac{2^{n+\frac{5}{2}}e^{-\frac{2n}{3}}n!\left|H_n\left(i\sqrt{\frac{2n}{3}}\right)\right|}{3^{n+1}(2n)!\left[1+(-1)^n e^{-2n}\right]}\approx 1-0.03/n. \tag{27}$$

The probability to detect n photons is

$$P(n)=\int|\Psi_n(x)|^2\,dx=\frac{\sqrt{2}(2n)!}{4^n(n!)^2}t^n(t+2)^{-n-\frac{1}{2}},\ t=g^2\frac{\Delta_2}{\Delta_1}. \tag{28}$$

When $t=4n$, $P(n)$ has a maximum value given by

$$P_{\max}(n)=\frac{(2n)!}{2^n(n!)^2}\sqrt{\frac{1}{2n+1}}\left(\frac{n}{2n+1}\right)^n. \tag{29}$$

In Fig. 3a, b, the squeezed state $|S_{\Delta_1}\rangle_1$ can be regarded as the input state. From Eq. (26), we can realize Eq. (9) when the following conditions are satisfied,

$$\sigma_{22}=1,\ \Delta_c^2=\frac{1}{|\sigma|+\sigma_{11}}=\Delta_1^2. \tag{30}$$

Let us derive a more specific expression for these conditions. The elements of σ can be easily obtained from the calculation rule of covariance matrices. In the case of Fig. 3a, the state $|G\rangle_{1,2}=\hat{B}|S_{\Delta_1}\rangle_1|S_{\Delta_2}\rangle_2$ gives

$$\sigma^{-1}=\begin{pmatrix}\sqrt{R}&-\sqrt{T}\\\sqrt{T}&\sqrt{R}\end{pmatrix}\begin{pmatrix}\Delta_1&0\\0&\Delta_2\end{pmatrix}\begin{pmatrix}\sqrt{R}&\sqrt{T}\\-\sqrt{T}&\sqrt{R}\end{pmatrix}=\begin{pmatrix}R\Delta_1+T\Delta_2&\sqrt{RT}(\Delta_1-\Delta_2)\\\sqrt{RT}(\Delta_1-\Delta_2)&T\Delta_1+R\Delta_2\end{pmatrix}, \tag{31}$$

$$\sigma=\begin{pmatrix}R\Delta_1^{-2}+T\Delta_2^{-2}&\sqrt{RT}\left(\Delta_1^{-2}-\Delta_2^{-2}\right)\\\sqrt{RT}\left(\Delta_1^{-2}-\Delta_2^{-2}\right)&T\Delta_1^{-2}+R\Delta_2^{-2}\end{pmatrix}. \tag{32}$$

Thus, Eq. (30) is given by

$$T\Delta_1^{-2}+R\Delta_2^{-2}=1,\ \Delta_2^{-2}=\frac{1}{1+\Delta_1^{-2}}. \tag{33}$$

Under these conditions, the process in Fig. 3a is given by Eq. (11). Similarly, in the case of Fig. 3b, the state $|G\rangle_{1,2}=\hat{S}_2(\Delta_3)\hat{Q}(g)|S_{\Delta_1}\rangle_1|S_{\Delta_2}\rangle_2$ gives

$$\sigma^{-1}=\begin{pmatrix}1&0\\0&\Delta_3^{-1}\end{pmatrix}\begin{pmatrix}1&g\\0&1\end{pmatrix}\begin{pmatrix}\Delta_1&0\\0&\Delta_2\end{pmatrix}\begin{pmatrix}1&0\\g&1\end{pmatrix}\begin{pmatrix}1&0\\0&\Delta_3^{-1}\end{pmatrix}=\begin{pmatrix}\Delta_1+g^2\Delta_2&g\Delta_2\Delta_3\\g\Delta_2\Delta_3&\Delta_2\Delta_3\end{pmatrix}, \tag{34}$$

$$\sigma=\begin{pmatrix}\Delta_1^{-2}&-g\Delta_1^{-2}\Delta_3^{-1}\\-g\Delta_1^{-2}\Delta_3^{-1}&\left(\Delta_2^{-2}+g^2\Delta_1^{-2}\right)\Delta_3^{-2}\end{pmatrix}. \tag{35}$$

Thus, Eq. (30) is given by

$$\left(\Delta_2^{-2}+g^2\Delta_1^{-2}\right)\Delta_3^{-2}=1,\ \Delta_1^{-2}\Delta_2^{-2}\Delta_3^{-2}=0. \tag{36}$$

Note that $\Delta_1^{-2}\Delta_2^{-2}\Delta_3^{-2}=0$ is unphysical, thus this condition should be approximately satisfied by assuming $\Delta_1^2\ll1\ll\Delta_2^2$ in addition to the former condition. With these conditions, the process in Fig. 3b is given by

$$\tilde{\mathcal{G}}_w[|S_\Delta\rangle]\approx\left[\hat{D}(-w)+\hat{D}(w)\right]|S_\Delta\rangle,\ w=\sqrt{2n}\Delta. \tag{37}$$

From the above, both setups in Fig. 3a, b can realize Eq. (9). However, only Fig. 3b satisfies Eq. (10), as discussed in the main text.

DATA AVAILABILITY

All data needed to evaluate the conclusions is available on figshare, 10.6084/m9.figshare.24166077.

Received: 8 June 2023; Accepted: 27 September 2023;
Published online: 10 October 2023

REFERENCES

1. Gottesman, D. An introduction to quantum error correction and fault-tolerant quantum computation https://arxiv.org/abs/0904.2557 (2009).

2. Gottesman, D. Fault-tolerant quantum computation with higher-dimensional systems. In *Quantum Computing and Quantum Communications* (eds. Williams, C. P.) 302–313 (Springer Berlin Heidelberg, 1999).
3. Fowler, A. G., Mariantoni, M., Martinis, J. M. & Cleland, A. N. Surface codes: towards practical large-scale quantum computation. *Phys. Rev. A* **86**, 032324 (2012).
4. Preskill, J. Quantum computing in the NISQ era and beyond. *Quantum* **2**, 79 (2018).
5. Arute, F. et al. Quantum supremacy using a programmable superconducting processor. *Nature* **574**, 505–510 (2019).
6. Gottesman, D., Kitaev, A. & Preskill, J. Encoding a qubit in an oscillator. *Phys. Rev. A* **64**, 012310 (2001).
7. Bravyi, S. & Kitaev, A. Universal quantum computation with ideal clifford gates and noisy ancillas. *Phys. Rev. A* **71**, 022316 (2005).
8. Knill, E. Quantum computing with realistically noisy devices. *Nature* **434**, 39–44 (2005).
9. Baragiola, B. Q., Pantaleoni, G., Alexander, R. N., Karanjai, A. & Menicucci, N. C. All-gaussian universality and fault tolerance with the Gottesman-Kitaev-Preskill code. *Phys. Rev. Lett.* **123**, 200502 (2019).
10. Yamasaki, H., Matsuura, T. & Koashi, M. Cost-reduced all-gaussian universality with the gottesman-kitaev-preskill code: resource-theoretic approach to cost analysis. *Phys. Rev. Res.* **2**, 023270 (2020).
11. Flühmann, C. et al. Encoding a qubit in a trapped-ion mechanical oscillator. *Nature* **566**, 513–517 (2019).
12. Campagne-Ibarcq, P. et al. Quantum error correction of a qubit encoded in grid states of an oscillator. *Nature* **584**, 368–372 (2020).
13. Larsen, M. V., Guo, X., Breum, C. R., Neergaard-Nielsen, J. S. & Andersen, U. L. Deterministic generation of a two-dimensional cluster state. *Science* **366**, 369–372 (2019).
14. Asavanant, W. et al. Generation of time-domain-multiplexed two-dimensional cluster state. *Science* **366**, 373–376 (2019).
15. Larsen, M. V., Guo, X., Breum, C. R., Neergaard-Nielsen, J. S. & Andersen, U. L. Deterministic multi-mode gates on a scalable photonic quantum computing platform. *Nat. Phys.* **17**, 1018–1023 (2021).
16. Asavanant, W. et al. Time-domain-multiplexed measurement-based quantum operations with 25-mhz clock frequency. *Phys. Rev. Appl.* **16**, 034005 (2021).
17. Harder, G. et al. Single-mode parametric-down-conversion states with 50 photons as a source for mesoscopic quantum optics. *Phys. Rev. Lett.* **116**, 143601 (2016).
18. Becerra, F. E., Fan, J. & Migdall, A. Photon number resolution enables quantum receiver for realistic coherent optical communications. *Nat. Photonics* **9**, 48–53 (2015).
19. Zhong, H.-S. et al. Quantum computational advantage using photons. *Science* **370**, 1460–1463 (2022).
20. Madsen, L. S. et al. Quantum computational advantage with a programmable photonic processor. *Nature* **606**, 75–81 (2020).
21. Vasconcelos, H. M., Sanz, L. & Glancy, S. All-optical generation of states for "Encoding a qubit in an oscillator". *Opt. Lett.* **35**, 3261–3263 (2010).
22. Weigand, D. J. & Terhal, B. M. Generating grid states from Schrödinger-cat states without postselection. *Phys. Rev. A* **97**, 022341 (2018).
23. Su, D., Myers, C. R. & Sabapathy, K. K. Conversion of gaussian states to non-gaussian states using photon-number-resolving detectors. *Phys. Rev. A* **100**, 052301 (2019).
24. Sabapathy, K. K., Qi, H., Izaac, J. & Weedbrook, C. Production of photonic universal quantum gates enhanced by machine learning. *Phys. Rev. A* **100**, 012326 (2019).
25. Tzitrin, I., Bourassa, J. E., Menicucci, N. C. & Sabapathy, K. K. Progress towards practical qubit computation using approximate Gottesman-Kitaev-Preskill codes. *Phys. Rev. A* **101**, 032315 (2020).
26. Fukui, K. et al. Efficient backcasting search for optical quantum state synthesis. *Phys. Rev. Lett.* **128**, 240503 (2022).
27. Takase, K., Yoshikawa, J., Asavanant, W., Endo, M. & Furusawa, A. Generation of optical Schrödinger cat states by generalized photon subtraction. *Phys. Rev. A* **103**, 013710 (2021).
28. Dakna, M., Anhut, T., Opatrný, T., Knöll, L. & Welsch, D.-G. Generating Schrödinger-cat-like states by means of conditional measurements on a beam splitter. *Phys. Rev. A* **55**, 3184–3194 (1997).
29. Filip, R., Marek, P. & Andersen, U. L. Measurement-induced continuous-variable quantum interactions. *Phys. Rev. A* **71**, 042308 (2005).
30. van Loock, P., Weedbrook, C. & Gu, M. Building gaussian cluster states by linear optics. *Phys. Rev. A* **76**, 032321 (2007).
31. Braunstein, S. L. Squeezing as an irreducible resource. *Phys. Rev. A* **71**, 055801 (2005).
32. Reck, M., Zeilinger, A., Bernstein, H. J. & Bertani, P. Experimental realization of any discrete unitary operator. *Phys. Rev. Lett.* **73**, 58–61 (1994).
33. Killoran, N. et al. Strawberry fields: a software platform for photonic quantum computing. *Quantum* **3**, 129 (2019).
34. Fukui, K., Tomita, A., Okamoto, A. & Fujii, K. High-threshold fault-tolerant quantum computation with analog quantum error correction. *Phys. Rev. X* **8**, 021054 (2018).
35. Glancy, S. & Knill, E. Error analysis for encoding a qubit in an oscillator. *Phys. Rev. A* **73**, 012325 (2006).
36. Ohliger, M., Kieling, K. & Eisert, J. Limitations of quantum computing with gaussian cluster states. *Phys. Rev. A* **82**, 042336 (2010).
37. Mari, A. & Eisert, J. Positive wigner functions render classical simulation of quantum computation efficient. *Phys. Rev. Lett.* **109**, 230503 (2012).
38. Vahlbruch, H., Mehmet, M., Danzmann, K. & Schnabel, R. Detection of 15 dB squeezed states of light and their application for the absolute calibration of photoelectric quantum efficiency. *Phys. Rev. Lett.* **117**, 110801 (2016).
39. Kashiwazaki, T. et al. Fabrication of low-loss quasi-single-mode PPLN waveguide and its application to a modularized broadband high-level squeezer. *Appl. Phys. Lett.* **119**, 251104 (2021).
40. Lita, A. E., Miller, A. J. & Nam, S. W. Counting near-infrared single-photons with 95% efficiency. *Opt. Express* **16**, 3032–3040 (2008).
41. Fukuda, D. et al. Titanium-based transition-edge photon number resolving detector with 98 fiber coupling. *Opt. Express* **19**, 870–875 (2011).
42. Gerrits, T. et al. Generation of optical coherent-state superpositions by number-resolved photon subtraction from the squeezed vacuum. *Phys. Rev. A* **82**, 031802 (2010).
43. Endo, M. et al. Non-gaussian quantum state generation by multi-photon subtraction at the telecommunication wavelength. *Opt. Express* **31**, 12865–12879 (2023).
44. Rančić, M., Hedges, M. P., Ahlefeldt, R. L. & Sellars, M. J. Coherence time of over a second in a telecom-compatible quantum memory storage material. *Nat. Phys.* **14**, 50–54 (2018).
45. Gerrits, T. et al. Extending single-photon optimized superconducting transition edge sensors beyond the single-photon counting regime. *Opt. Express* **20**, 23798–23810 (2012).
46. Lamas-Linares, A. et al. Nanosecond-scale timing jitter for single photon detection in transition edge sensors. *Appl. Phys. Lett.* **102**, 231117 (2013).
47. Cahall, C. et al. Multi-photon detection using a conventional superconducting nanowire single-photon detector. *Optica* **4**, 1534–1535 (2017).
48. Zhu, D. et al. Resolving photon numbers using a superconducting nanowire with impedance-matching taper. *Nano Lett.* **20**, 3858–3863 (2020).
49. Endo, M. et al. Quantum detector tomography of a superconducting nanostrip photon-number-resolving detector. *Opt. Express* **29**, 11728–11738 (2021).
50. Joshi, C., Farsi, A., Clemmen, S., Ramelow, S. & Gaeta, A. L. Frequency multiplexing for quasi-deterministic heralded single-photon sources. *Nat. Commun.* **9**, 847 (2018).

ACKNOWLEDGEMENTS

This work was partly supported by the Japan Society for the Promotion of Science KAKENHI (18H05207, 20K15187, and 22K20351), the Japan Science and Technology Agency (JPMJMS2064), the BMBF in Germany (QR.X and PhotonQ), the EU/BMBF via QuantERA (ShoQC), and the Deutsche Forschungsgemeinschaft (DFG, German Research Foundation) - Project-ID 429529648 - TRR 306 QuCoLiMa ("Quantum Cooperativity of Light and Matter"). We acknowledge support from UTokyo Foundation and donations from Nichia Corporation of Japan. W.A. and M.E. acknowledge support from Research Foundation for OptoScience and Technology. A.K. acknowledges financial support from The Forefront Physics and Mathematics Program to Drive Transformation (FoPM). We would like to thank T. Mitani for careful proofreading of the manuscript.

AUTHOR CONTRIBUTIONS

K.T. conceived the protocol and conducted the simulation. K.T., K.F., A.K., W.A., M.E., J.-i.Y. and P.v.L. formulated the protocol. A.F. supervised the project. K.T. wrote the manuscript with assistance from all other coauthors.

COMPETING INTERESTS

The authors declare no competing interests.

ADDITIONAL INFORMATION

Correspondence and requests for materials should be addressed to Kan Takase or Akira Furusawa.